SYSTEMATIC UNCERTAINTIES ON MONTE CARLO SIMULATION OF LEAD BASED ADS

M. Embid
CIEMAT. Fission driven by Accelerator and Isotopes Transmutation
Avda. Complutense, 22 Edif.-17 Dpcho.101, 28040 Madrid
Spain

R. Fernández
CIEMAT. Fission driven by Accelerator and Isotopes Transmutation
Avda. Complutense, 22 Edif.-17 Dpcho.101, 28040 Madrid
Spain

J.M. García-Sanz
CIEMAT. Fission driven by Accelerator and Isotopes Transmutation
Avda. Complutense, 22 Edif.-55, 28040 Madrid
Spain

E. González
CIEMAT. Fission driven by Accelerator and Isotopes Transmutation
Avda. Complutense, 22 Edif.-17, 28040 Madrid
Spain

Abstract

Computer simulations of the neutronic behaviour of ADS systems foreseen for actinide and fission product transmutation are affected by many sources of systematic uncertainties, both from the nuclear data and by the methodology selected when applying the codes. Several actual ADS Monte Carlo simulations are presented, comparing different options both for the data and for the methodology, evaluating the relevance of the different uncertainties.

Introduction

This report shows a compilation of several exercises to evaluate sources of the systematic uncertainties on the predictions computed on ADS Montecarlo simulations, including:

A. Uncertainties in the estimation of K_{eff} of a lead based ADS from the nuclear cross section libraries: ENDF-BVI.4 vs. JENDL-3.2.

B. Sensitivity study for the K_{eff} of a lead based ADS on different proton beam window heights

C. Comparison of the fully detailed heterogeneous geometrical descriptions of a lead based ADS versus its simplified homogeneous description in MC neutronic calculations.

D. Sensitivity studies on lead based ADS with UO_2 fuel.

E. Sensitivity study on the spatial segmentation of lead based ADS geometry for burnup evolution simulation

A. Uncertainties in the estimation of K_{eff} of a lead based ADS from the Nuclear Cross Section Libraries: ENDF-BVI.4 vs. JENDL-3.2

In any simulation of the neutronic behaviour of a nuclear system, the accuracy of the results is limited by the precision of used nuclear databases, in particular for the cross sections. In the study of Accelerator Driven System (ADS) for transmutation, new elements in nuclear systems appear. The best example is the very important role played by unusual isotopes, particularly lead and some transuranids. In the present paper, the results of a comparison of the predicted behaviour of one Th-TRU and lead based ADS according to the ENDFB-6.4 and JENDL-3.2 databases will be presented.

The studied ADS configuration is based on: liquid lead coolant with natural convection, Th+TRU fuel and a thermal power of 250 MWth. For this study a simplified ADS model intended for TRU incineration has been selected. The main characteristics are: the use of a mixture of ThO_2 and transuranids dioxide as fuel and lead as cooling and diffusory material. More details on, fuel and geometrical parameters can be found in references [1,2].

K_{eff} dependence on the cross section database

For the ADS described in the previous paragraph, K_{eff} has been computed using the “kcode” module of the MCNP-4b [3] Monte Carlo code.

Three groups of simulations have been computed, each one corresponding to a different cross section database set. In case 1, the ENDFB-6.4 cross section has been used for all the isotopes, translated to ACE format using NJOY94.61 [4], at 750 K for the lead and at 1200 K for all the other isotopes. In case 2, the JENDL-3.2 cross sections are used for all the isotopes, also computed with the help of NJOY94.61 and at same temperatures as in case 1.

The third case is subdivided in several subcases, at each subcase the JENDL-3.2 cross sections database is used for all the isotopes except one or several isotopes. Table 1 describe the details of each case. In this way the individual effects of the Pb, ^{240}Pu, ^{239}Pu, ^{232}Th and Fe cross sections and the combined effects of Pb and ^{240}Pu on K_{eff} have been studied.

For each simulation, the K_{eff} value has been computed using the kcode module of MCNP-4b, running 50 cycles of 2000 fission neutrons each. The K_{eff} estimators were computed over the last 45 cycles, skipping the events of the first five. The starting fission source is given by a SRCTP file produced in a previous MCNP-4b run using the same input file. At the end of each run, MCNP checks that every cell containing fissile material has been sampled.

Table A-1. **Simulated cases with MCNP-4b**.

Case	Isotope	New Library	Temp. (^{0}K)
1	All	ENDFB-6.4	-
2	All	JENDL-3.2	-
3.1	All JENDL3.2 except Pb nat.		
	^{206}Pb (24.44%)	ENDFB-6.4	750
	^{207}Pb (22.42%)	ENDFB-6.4	750
	^{208}Pb (53.14%)	ENDFB-6.4	750
3.2	All JENDL3.2 except		
	Pb-isotopic mixture	ENDFB-6.4	750
	^{240}Pu	ENDFB-6.4	1200
3.3	All JENDL3.2 except ^{240}Pu	ENDFB-6.4	1200
3.4	All JENDL3.2 except ^{232}Th	ENDFB-6.4	1200
3.5	All JENDL3.2 except ^{239}Pu	ENDFB-6.4	1200
3.6	All JENDL3.2 except Fe-nat		
	^{54}Fe (5.84%)	ENDFB-6.4	1200
	^{56}Fe (91.75%)	ENDFB-6.4	1200
	^{57}Fe (2.12%)	ENDFB-6.4	1200
	^{58}Fe (0.28%)	ENDFB-6.4	1200

The final K_{eff} selected is a statistical combination [3] of three individual estimators: collision, absorption and track-length. The values of the different estimators and the final combined result for K_{eff} in the different cases studied are shown in table A-2.

Table A-2 **Value of the K_{eff} in each studied case**

	K_{eff} estimators				
Case	**$K_{coll.}$**	**$K_{abs.}$**	**K_{tl}**	**K_{eff}**	**Standard deviation**
1	0.9606	0.9609	0.9607	0.9607	0.002
2	0.9445	0.9445	0.9454	0.9444	0.002
3.1.	0.9670	0.9699	0.9672	0.9677	0.002
3.2.	0.9708	0.9667	0.9710	0.9692	0.002
3.3.	0.9441	0.9441	0.9440	0.9441	0.002
3.4.	0.9349	0.9364	0.9344	0.9349	0.002
3.5.	0.9401	0.9377	0.9404	0.9392	0.001
3.6.	0.9408	0.9405	0.9411	0.9409	0.002

A large difference, 0.016 ± 0.003, is observed in the predicted value of K_{eff} using ENDF (case 1) versus JENDL (case 2) libraries. This difference would induce a 30% difference in the neutronic multiplication. The largest contribution come from lead, cases 3.1 and 3.2. In fact the ENDF databases for lead alone will produce an even larger difference, 0.023 ± 0.003. This difference is slightly compensated by the ^{232}Th cross sections, case 3.4. Changing the ^{239}Pu, ^{240}Pu or Fe cross sections databases, the calculated K_{eff} is not modified significantly. In the following paragraphs the difference on the lead cross sections are analysed in order to identify the origin of the discrepancy in the K_{eff} estimation.

Main lead cross sections (JENDL-3.2 and ENDFB-6.4).

Total, elastic, inelastic, (n,2n), (n,3n) and capture, the more relevant cross sections for lead, are shown in figure A-1.

There are very small differences on total, elastic scattering and capture cross sections of lead between the two libraries, JENDL-3.2 and ENDFB-6.4. On other hand, there are significant differences on the (n,2n) and (n,3n) cross sections but only for energies above 10 MeV.

The largest differences appear on the inelastic scattering reactions. Due to its large cross section between 1 and 10 MeV, the inelastic reactions are the dominant non-elastic process at these energies. In this range the values provided by JENDL-3.2 are always higher than the corresponding to ENDFB-6.4, figure A-2, for all the lead isotopes. In addition secondary neutrons energies are computed with different algorithms.

Figure A-1. **Main neutron cross sections for natural lead (JENDL-3.2).**

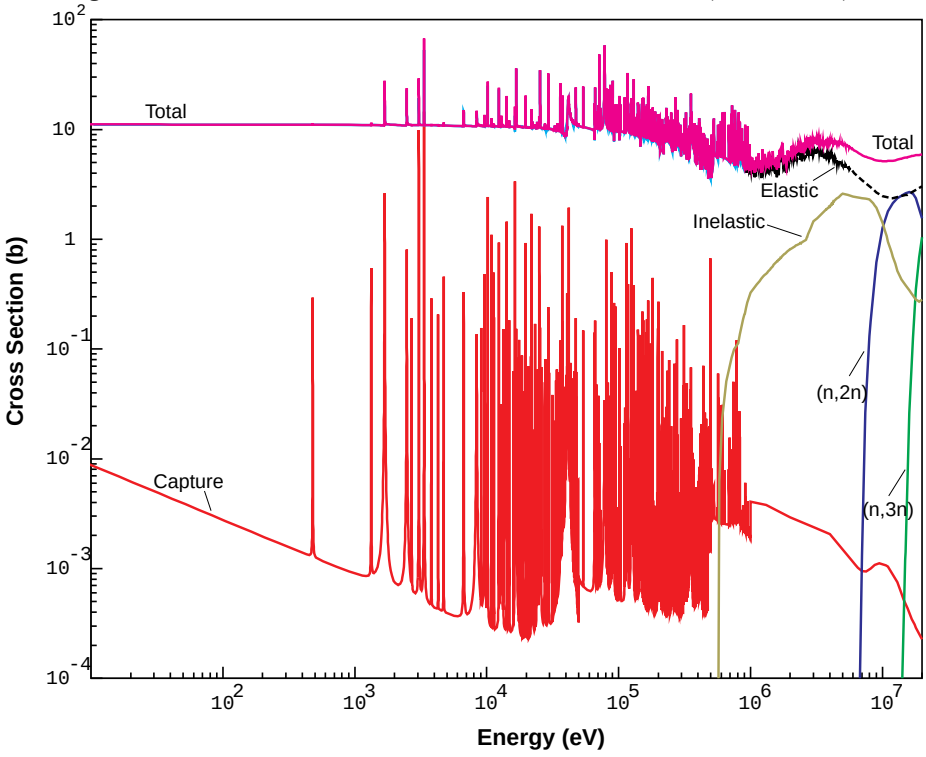

Figure A-2. **Inelastic-scattering cross section for ^{208}Pb and ^{207}Pb (JENDL-3.2 - ENDFB-6.4)**

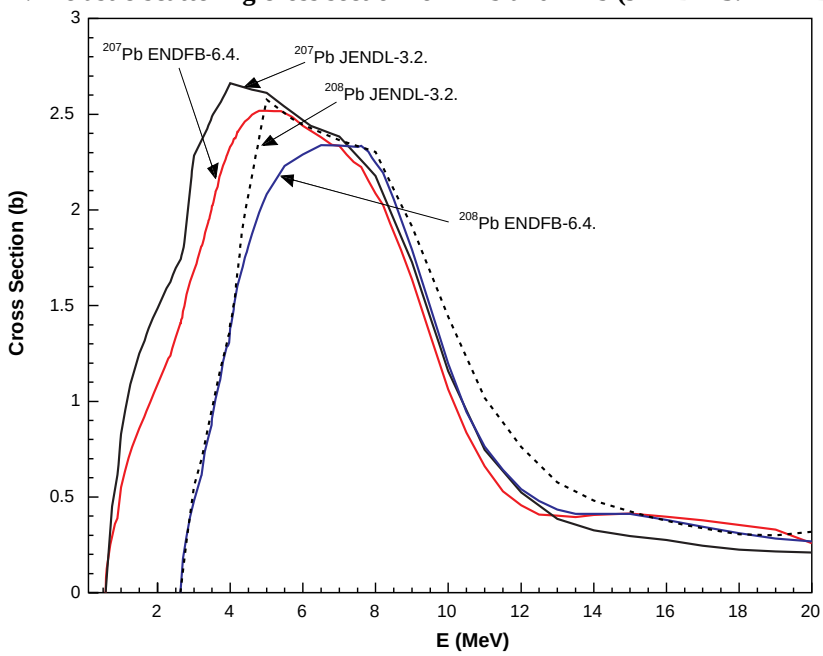

Analysis of the results.

According to the previous section and taking into account the neutron flux energy spectra, the largest differences should come from the inelastic scattering cross section of lead. In figure A-3 two graphs are shown: the average neutron fluences and the inelastic-scattering cross sections of core material, for the two libraries. Figure A-4 displays the ratios between both nuclear databases for the graphs of figure A-3.

Figure A-3. **Differences on the average core neutron fluence and on the inelastic cross section for JENDL-3.2 versus ENDFB-6.4**

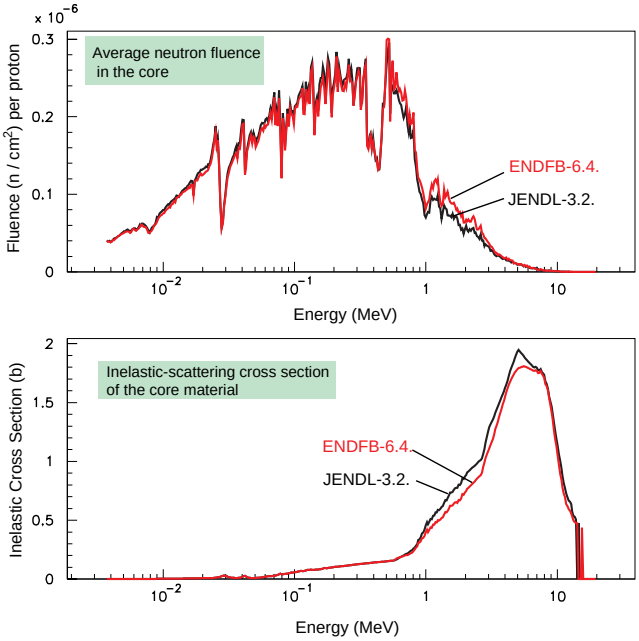

Figure A-4. **Ratios of the comparisons JENDL-3.2 versus ENDFB-6.4 of the previous figure**

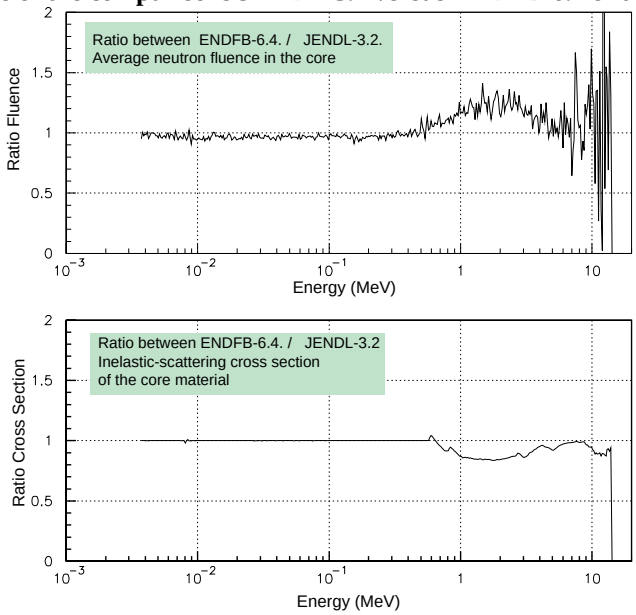

The conclusion from the last figures is that the higher inelastic scattering rate predicted by the JENDL-3.2 database sends more neutrons, from the energy range between 500 keV and 20 MeV, directly to lower energies. Figure A-5 shows that for the Th+TRUs mixture of the ADS core, fission dominates clearly over capture in that energy range whereas capture dominates over fission at lower energies, for both databases. The obvious result is that a larger fission rate and consequently a larger K_{eff} are predicted by ENDF.

Figure A-5. **Capture, fission and inelastic-scattering cross sections for the ADS core material with both libraries**

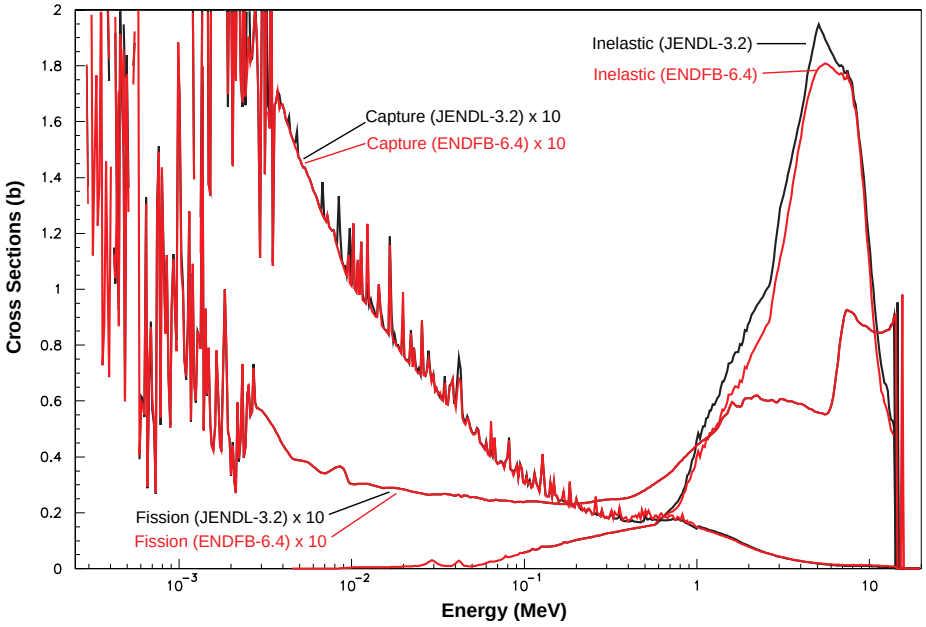

Evaluated versus experimental cross section data

The figure A-6 shows the comparison between the evaluated inelastic-scattering cross section by both nuclear databases and the EXFOR-97 [5] experimental data (non-elastic cross-sections).

The data available are clearly insufficient for making a choice. It should be noted, however, that experimental points not available in EXFOR-97 have been used in both the JENDL-3.2 and the ENDFB-6.4 evaluations.

Figure A-6 **Evaluated inelastic scattering cross section of lead from JENDL-3.2 and ENDFB-6.4 versus experimental data (EXFOR-97)**

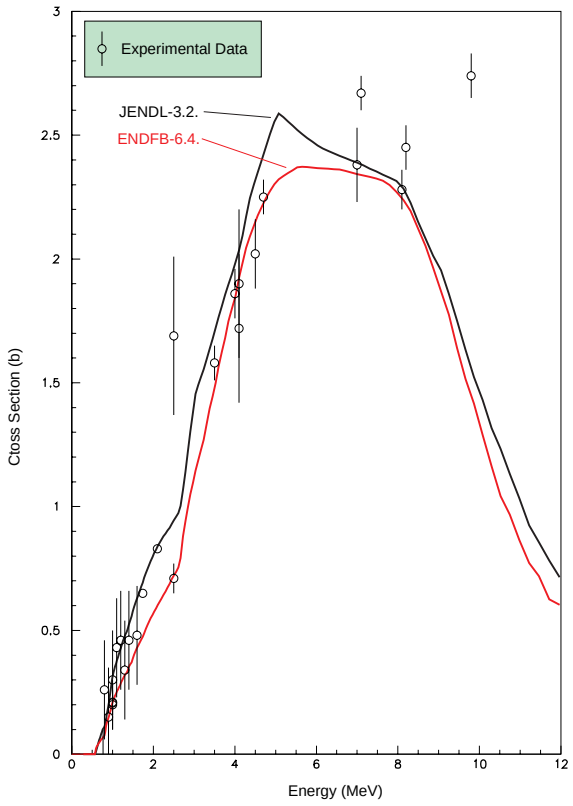

Conclusions of exercise A

According to JENDL-3.2 database the inelastic scattering with lead sends more neutrons, from the energy range between 500 keV and 20 MeV, directly to lower energies, than in simulations using ENDF-BVI.4. Fission dominates clearly over capture in the high energy range whereas capture dominates over fission at lower energies, for both databases. The obvious result is that a larger fission rate and consequently a larger K_{eff} are predicted by ENDF.

Unfortunately the available experimental data do not appear to be sufficient to make a clear choice. In the present situation this uncertainty has to be taken into account in the predictions of lead based ADS.

On the other hand it would be very interesting to have extra experimental data to enable more precise evaluations.

B. Sensitivity study for the K_{eff} of a lead based ADS on different proton beam window heights

The performance of an Accelerator Driven System (ADS), is conditioned by the optimisation of the geometrical coupling between the accelerator and the subcritical nuclear assembly. The aim of this exercise is to study the sensitivity to this parameter and to find an optimisation for a given ADS configuration. In the exercise [7], the position (height) of the beam window respect to the subcritical device core is modified in a large range. The other parameters of the ADS remain fixed.

The ADS set-up correspond to the case described in the references [2,3], but with a variable height of the beam window respect to the subcritical device core. These references also describes the MCNP and libraries versions used to simulate the neutron transport below 20 MeV. The proton beam interaction with lead, the neutron production by spallation and the transport of these neutrons down to 20 MeV is done with the help of LAHET [6].

In all the cases considered the protons in the beam have a kinetic energy of 400 MeV. In the exercise, the window height has been varied from -30 cm (down) to 60 cm (up) respect for the centre of the subcritical device core. Figure B-2 shows the neutron multiplication constant, K_s, for the different positions of the beam window. In all cases the neutron source is defined as the set of neutrons produced by the proton beam, stopped as soon as the neutron energy is smaller than 20 MeV. A wide flat region is observed between 5 cm and 35 cm above the centre of the subcritical device core. Outside this region, the K_s decreases.

Figure B-1. **Side view of the ADS. Searching of the optimal height of the neutronic spallation source**

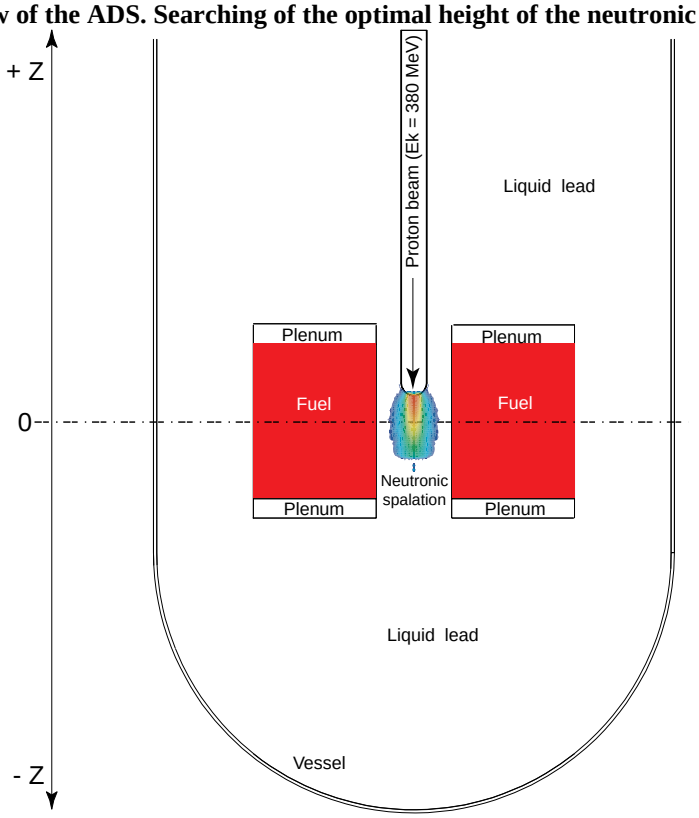

Figure B-2 **K_s variation versus the height of the beam window respect to the core centre**

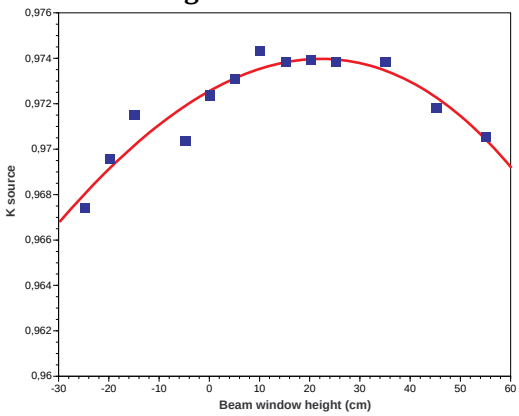

C. Comparison of the fully detailed heterogeneous geometrical descriptions of a lead based ADS versus its simplified homogeneous description in MC neutronic calculations

The need of computer time reduction in the Montecarlo (MC) simulations and the fact that the mean collision length is larger than the distance between pins in the typical accelerator driven subcritical fission device, ADS, has leaded to use homogeneous approximations of the detailed geometry in many studies of this type of devices.

In this paper two geometry models, from a larger study [8,9] of the EA-1500 (Energy Amplifier of 1500 MWth) have been compared:

1. A complete geometry definition of each fuel pin (including plenums, cladding and void) (Heterogeneous model).
2. Homogeneous mixture of the material of each bundle, distributed over its complete volume.

All the simulations were performed with the help of MCNP4b for the neutron transport and evaluation of the criticality of the system. LAHET was used when it was necessary to simulate the interaction of the protons from the accelerator with the spallation target. The main characteristics of the fuel bundles of the ADS for this study are shown in table C-1 and the core geometries as presented in figures C-1 and C-2.

Table C-1 **Main Characteristics of the fuel bundles**

	Inner Core	**Outer Core**	**Breeder**
Flat to flat (mm)	234	234	234
Thickness of the wall bundle (mm)	3	3	3
Distance between fuel pins (mm)	12.43	11.38	11.38
Number of bundles	30	90	42
Number of fuel pins in a bundle	331	397	397
Material of the wall bundle	HT9	HT9	HT9
Coolant/Moderator	Pb	Pb	Pb
Fuel Composition	ThO_2+UO_2	ThO_2+UO_2	ThO_2

Figure C-1. **Top view of the homogeneous EA-1500 core**

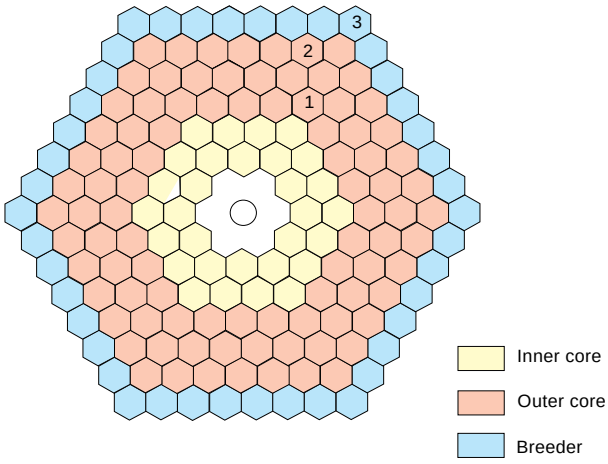

Figure C-2. **Full detailed geometry (Heterogeneous model) of the simulated ADS by MCNP-4b. The differences in the neutron energy distribution of the fluence for the heterogeneous and homogeneous model are shown in figure C-3 and C-4 as function of the energy**

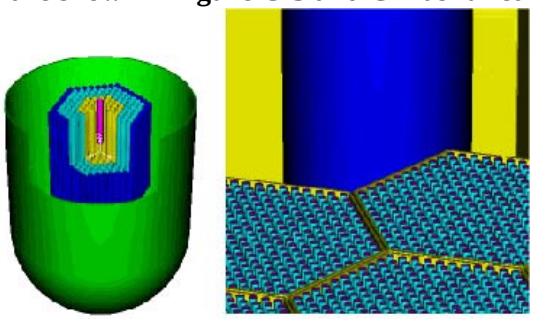

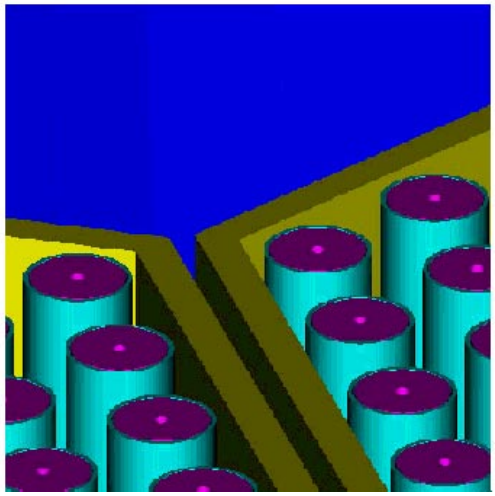

Figure C-3 **Homogeneous / heterogeneous fuel fluences: Inner core**

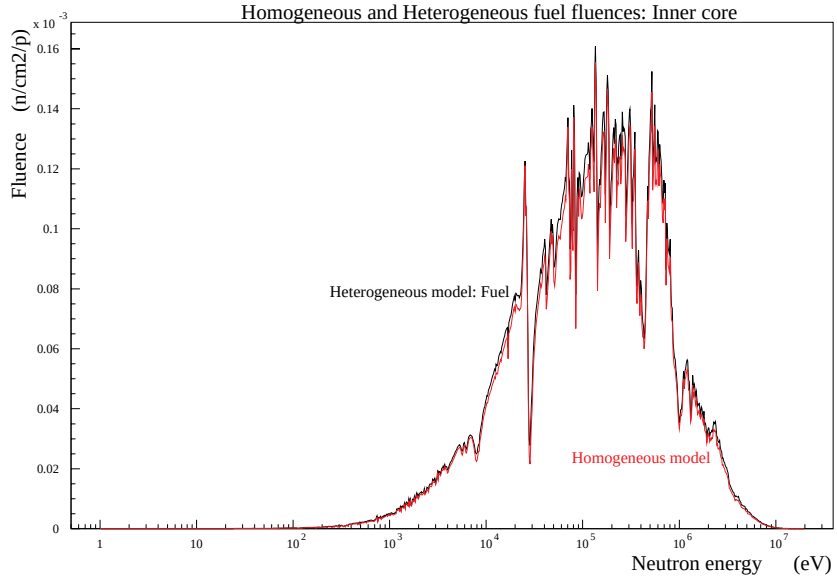

Figure C-4 **Homogeneous / heterogeneous fuel fluences ratio: Inner core**

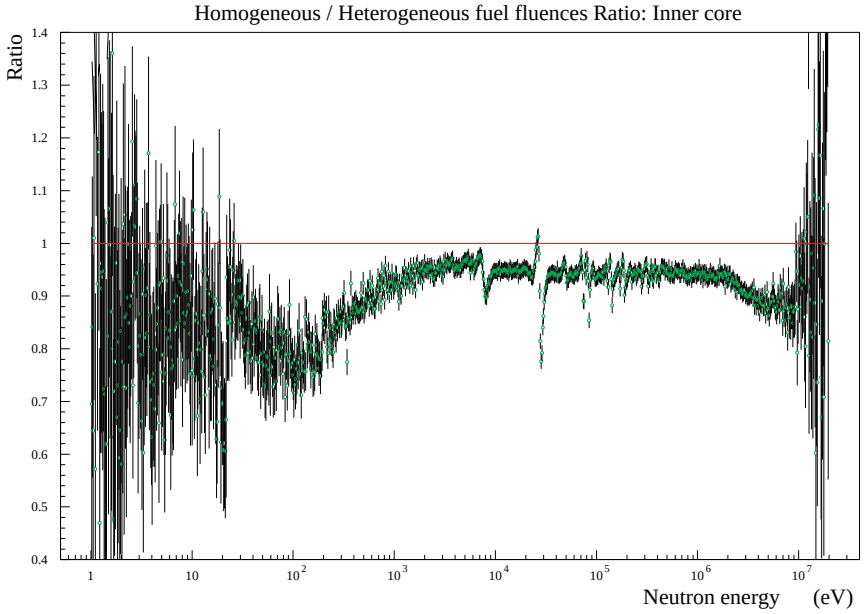

The fact that the ratio between the fluence and reaction rates between the two geometries are nearly independent of the neutron energy suggests that the difference is coming from the total neutron population. As the spallation source is expected to be nearly identical, the multiplication in the subcritical device should produce the observed difference.

The Keff has been computed for both geometries using the KCODE procedure of the MCNP code. In principle, the expected multiplication should be 1/(1-Keff), however as the fission source distribution produced by the spallation process is different from the eigen function of the transport equation, the net multiplication for a spallation source is slightly different. The values obtained from MCNP are shown in table C-2.

Table C-2:

	K_{eff}	Multiplication $1/(1-K_{eff})$	Net Multiplication (spallation source included)
Heterogeneous	0.9559±0.0009	22.7±0.5	25.6±0.3
Homogeneous	0.9505±0.0011	20.2±0.5	23.8±0.2

The resulting ratio homogeneous over heterogeneous in the net multiplication is 0.930 ± 0.014 which is in good agreement with the ratios obtained for the fluences and reaction rates, shown in tables C-3 and C-4.

Table C-3 **Average flux and energy produced by fission on each core zone for both LAHET/MCNP simulations**.

Flux (n/cm^2/proton)		**BR**	σ_{rel}	**OC**	σ_{rel}	**IC**	σ_{rel}
Heterogeneous	Fuel	3.58×10^{-3}	0.014	1.42×10^{-2}	0.014	3.25×10^{-2}	0.012
	Cladding	3.59×10^{-3}	0.014	1.42×10^{-2}	0.014	3.25×10^{-2}	0.012
	Lead	3.59×10^{-3}	0.014	1.42×10^{-2}	0.014	3.25×10^{-2}	0.012
Homogeneous		3.28×10^{-3}	0.010	1.31×10^{-2}	0.009	3.06×10^{-2}	0.008
Ratio (homogeneous/ heterogeneous fuel)		0.916	0.017	0.922	0.017	0.942	0.014
Fission energy produced (MeV/p)		**BR**	σ_{rel}	**OC**	σ_{rel}	**IC**	σ_{rel}
Heterogeneous		—	—	33719	0.014	21749	0.012
Homogeneous		—	—	31103	0.009	20414	0.008
Ratio (homogeneous/ heterogeneous fuel)		—	—	0.922	0.017	0.939	0.014

Table C-4 **Average capture rate of ^{232}Th and fission rate of ^{233}U on each core zone for both LAHET/MCNP simulations**

^{232}Th capture rate (capt/p)	**BR**	σ_{rel}	**OC**	σ_{rel}	**IC**	σ_{rel}
Heterogeneous	40.0	0.014	208.0	0.014	136.0	0.012
Homogeneous	37.0	0.009	193.3	0.009	129.0	0.008
Ratio (homog./ heterog.)	0.925	0.017	0.929	0.017	0.949	0.014
^{233}U fission rate (fiss/p)	**BR**	σ_{rel}	**OC**	σ_{rel}	**IC**	σ_{rel}
Heterogeneous	—	—	181.4	0.014	117.3	0.012
Homogeneous	—	—	167.4	0.009	110.2	0.008
Ratio (homog./ heterog.)	—	—	0.923	0.017	0.939	0.014

Conclusions of exercise C

Small but statistically significative differences on the fluences and in the main reaction rates are obtained, 5 to 9% depending on the core region, when comparing the homogeneous and heterogeneous models. Apart from few resonances of the cladding materials, the ratio of the results for the two geometrical descriptions is almost neutron energy independent.

This difference can be explained by a small difference on the effective multiplication factor, coming both from the small difference on the volume the fissile material is distributed over, and the different distribution of isotopes on the available volume.

However, in additional studies [8,9] it has been demonstrated that an homogeneous model with simple modifications can be adapted to provide acceptable description of the ADS behaviour on most usual studies.

D. Sensitivity studies on lead based ADS with UO_2 fuel

The present study shows the different estimations on Keff of an ADS-250, lead cooled, when using heterogeneous or homogeneous geometry description and different databases, for UO_2 fuels with different enrichments on ^{235}U. More details studies can be found at references [10,11,12]. The ADS geometry is always the same as in exercises A-C.

Different types of fuel have been considered in the neutronic simulation of ADS. In particular, for the first stages of a demonstration plant, it is presumably desirable a well-known fuel to be used. According to this, preliminary studies of the neutronic characteristics of a moderately enriched uranium dioxide ADS have been performed.

Several simulations had been performed both with fully detailed geometries (heterogeneous) and with simplified homogeneous geometries, using in each case first the JENDL-3.2 and second the ENDFB-VI.4 the nuclear data libraries. The results of the different simulations corresponding to different ^{235}U enrichments are shown on table D-1. These results, show a difference of up to 2 % between both libraries, owing to the differences in the lead elastic cross-section, ^{2}. The most important conclusion is that because the uncertainties associated to the method and cross section data libraries conservatives designs should be used. For example, a 18 % UO_2 enrichment gives a subcritical keff of 0.990 in a homogeneous simulation with JENDL3.2 data library, but it rises up to critical (1.012) in a heterogeneous simulation with ENDFB-VI R.4 data library.

Table D-1 **Keff vs. enrichment with different cross section data libraries and heterogeneous and homogeneous simulation**

% enrichment	**K_{eff} (JENDL3.2) homogeneous**	**K_{eff} (JENDL3.2) heterogeneous**	**K_{eff} ENDFBVI-R.4 homogeneous**	**K_{eff} ENDFBVI-R.4 heterogeneous**
10%	0.715±0.001	0.723±0.001	0.735±0.001	0.744±0.001
17%	0.961±0.02	0.967±0.001	0.982±0.001	0.985±0.001
18%	0.990±0.002	0.995±0.001	1.009±0.001	1.012±0.001

E. Sensitivity study on the spatial segmentation of lead based ADS geometry for burnup evolution simulation

Independently of the detail geometry of the ADS for the neutron transport calculation, a segmentation of the elements or groups of elements of the ADS core is required for burnup material evolution simulation.

The spatial dependence on the neutron flux intensity and its energy dependence inside the core, implies that a complete core fuel depletion calculation performed in zero-dimension approach could give inadequate results. Defining a core division in regions of almost constant reaction rates, several zero-dimension fuel burn up calculations can be performed. The ulterior addition of results will bring the time evolution of the full core taking into account the geometry dependencies [13,14]. The ideal limit is an extremely fine core division, but this will mean a very large amount of depletion calculations. In our simulations we have divided the core in 10 different longitudinal zones. In total (120 fuel assemblies x 10) there are 1200 zones. Symmetric fuel assemblies are grouped for the material evolution simulations resulting only 140 independent cells.

In this paper we perform a study of the characteristics of the reaction rates of different isotopes in order to estimate the error from this spatial segmentation, and to achieve an equilibrium between computing time and simulation errors.

The calculated reaction rates can be separated into two factors: the so-called one group cross section (which means energy integrated, weighted by the proper flux spectrum) and the integrated flux. While the flux depends on the position and not on the studied reaction, the cross section in one group has nearly no dependence on the position.

The fuel assemblies in the core are divided in six groups of symmetric fuel assemblies, each of them are composed by 14 fuel assemblies. The figure E-1 shows the structure of the core identifying by labels, the groups of symmetric assemblies.

Figure E-1 **Structure of the core of the simulated ADS. The numbers identify groups of symmetric assemblies**

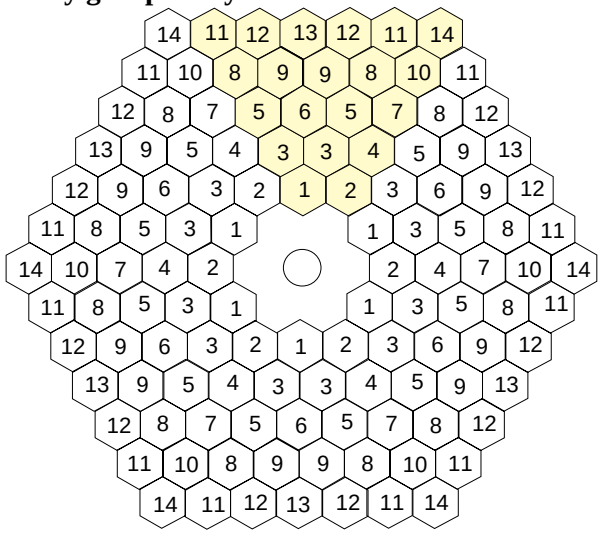

The comparison of the reaction rates of the most important isotopes on the different subcells (140 in total), allows to estimate their dependence with the position in the core, both along XY and Z. Figure E-2 shows the estimated maximum relative error in the concentration of ^{232}Th at any point within each subcells from the XY gradient of the evolution, after 1400 days of evolution at a total thermal power of 800 MW (average burnup of 120 GWd/HMT). This error is computed as half the maximum difference between the final concentration at one subcell and any of its neighbours. Figure E-3 presents the estimated maximum relative error in the ^{232}Th concentration due to the Z gradients, and Figure E-4 and E-5 the corresponding maximum relative errors for the ^{239}Pu concentrations.

Figure E-2. **Maximum relative error in the concentration of ^{232}Th, from the XY gradients of the reaction rates**

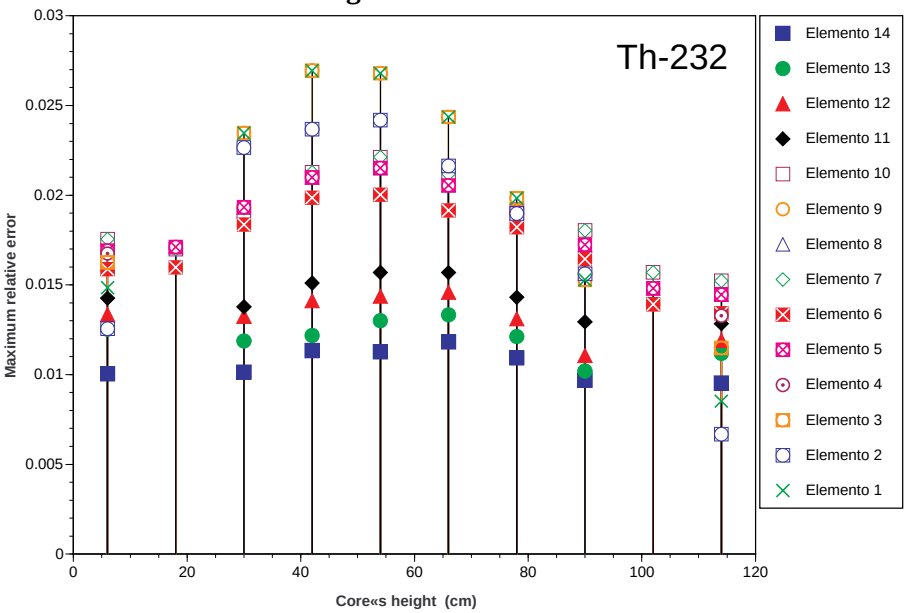

Figure E-3. **Maximum relative error in the concentration of ^{232}Th, from the Z gradients of the reaction rates**

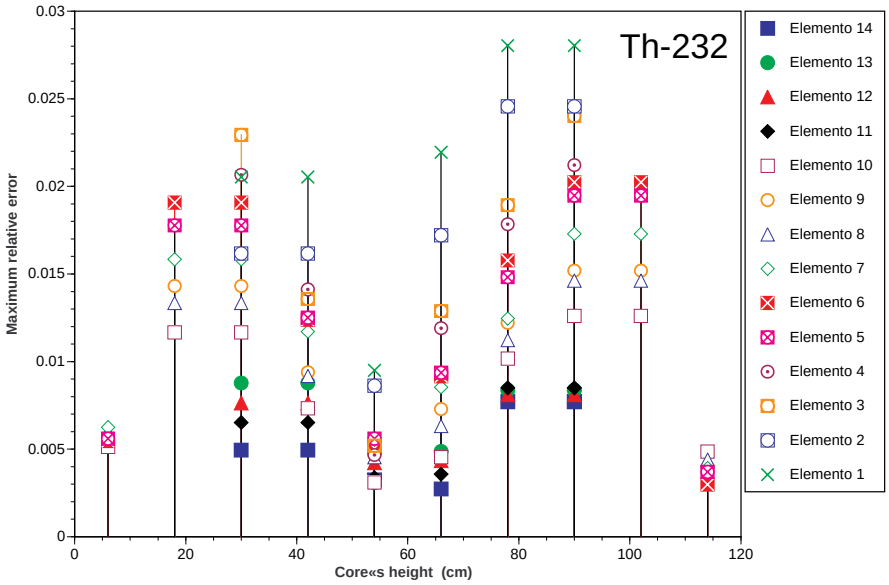

Figure E-4 **Maximum relative error in the concentration of ^{239}Pu, from the XY gradients of the reaction rates**

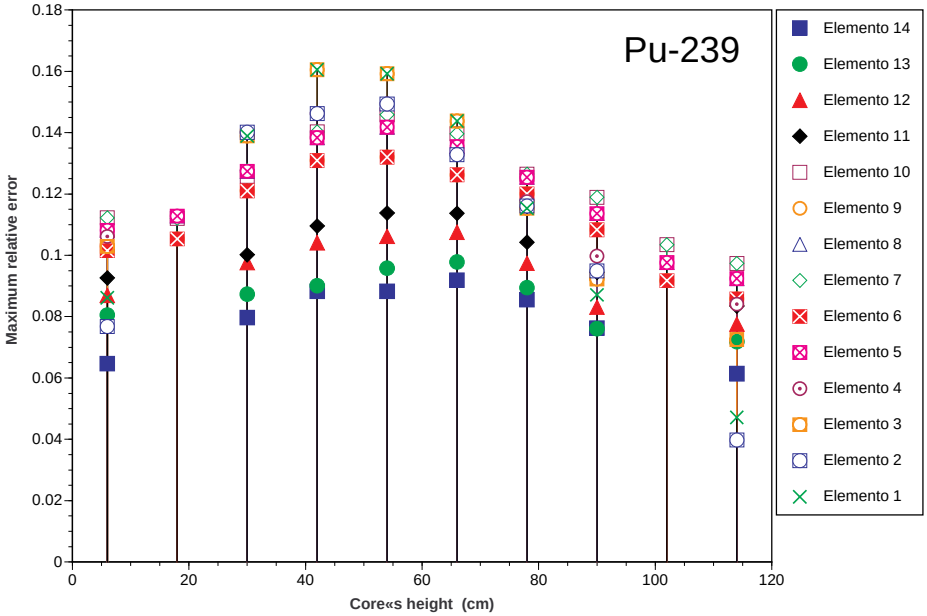

Figure E-5 **Maximum relative error in the concentration of ^{239}Pu, from the Z gradients of the reaction rates**

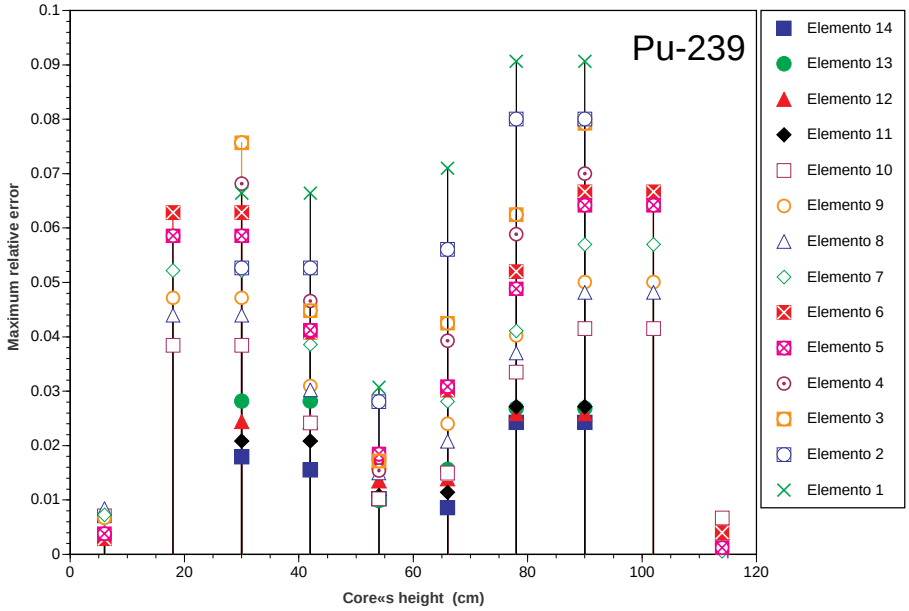

Figure E-6. **Reaction rate map per atom per second, close to the middle plane of the core**

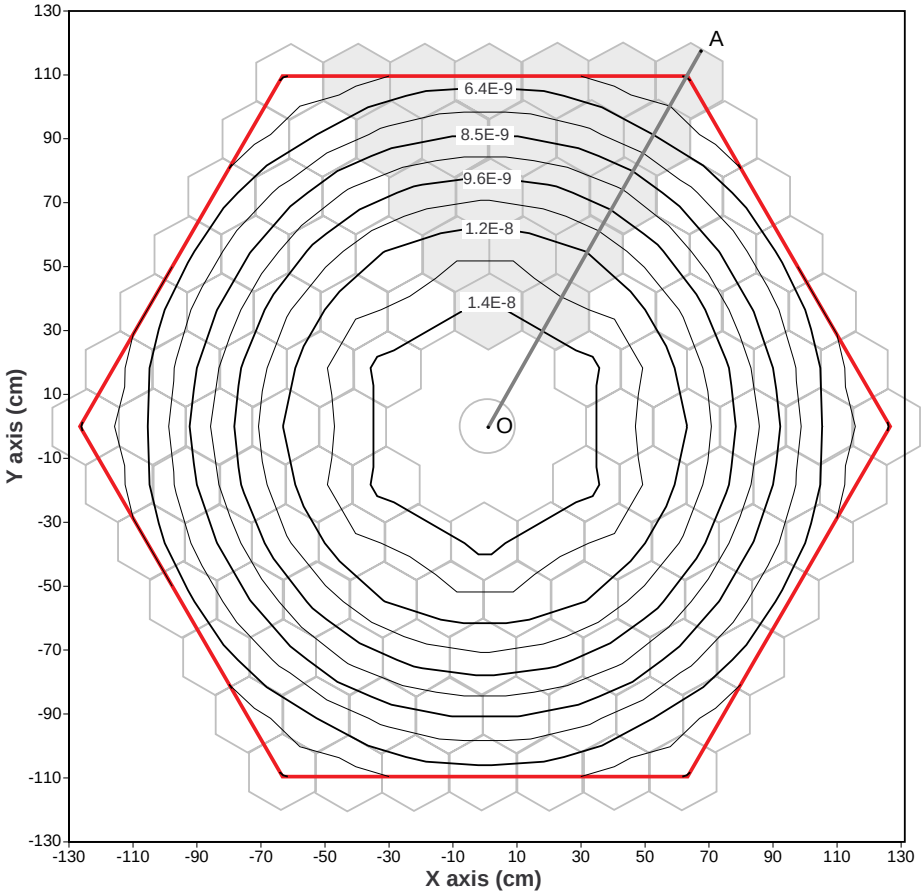

This error already moderated in magnitude have different signs for different positions within each subcell, and large compensations appear when computing the evolution of the material of the complete subcell or of the full system as a whole, reducing the final estimation error on the discharge isotopic composition. To estimate the error on the prediction for the material evolution of a subcell we have evaluated the map of reaction rates of fission and capture in ^{239}Pu, Figure E-6, and in particular the non linearity of these reaction rates along the O-A line of that figure. The results shown in Figure E-7, allow to estimate that the global error on the ^{239}Pu average concentration on the subcells is smaller than 0.4%.

Conclusions of exercise E

In order to prepare an isotopic-concentration time evolution calculation of an ADS, a core geometry segmentation must be done, dividing it into cells of almost constant reaction rates.

For a subcritical device such as our simulated ADS, the granularity in this division is mainly forced by the gradients of the flux in the core.

In our case dividing the core in 140 different zones (10 axial x 14 radial) we estimate an acceptable error (< 15%) in the reaction rates per atom along to the radial and axial directions, for individual fuel pins, and negligible errors for the average fuel subassembly composition evolution.

Figure E-7. **Radial distribution of the reaction rate per atom of Pu-239 along line O-A (Figure E-6)**

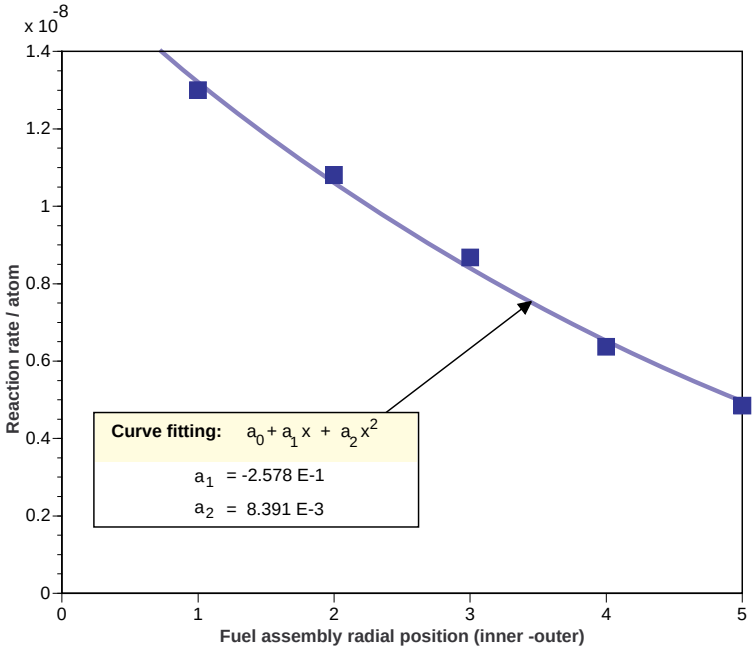

REFERENCES

[1] R.Fernández and E. González. Ejercicio de cálculo de la distribución de potencia específica de un diseño de Amplificador de Energía de 250 MW térmicos mediante LAHET/MCNP. CIEMAT/FACET/97-01.

[2] Embid, R. Fernández and E. González. Sensitivity study for the K_{eff} of a lead based ADS on the cross sections evaluations: ENDFB-6.4 and JENDL-3.2. CIEMAT REPORT 846 (1998).

[3] Briesmeister, Editor. MCNP™ - A General Monte Carlo N-Particle Transport Code. Version 4B. LA-12625 (1997).

[4] MacFarlane, D.W. Muir. The NJOY nuclear data processing system. Version 91. December 1994.

[5] EXFOR-97,Experimental Nuclear Reaction Data, IAEA.

[6] Prael and Henry Lichtenstein. User Guide to LCS: The LAHET Code System. LANL Group X-6 MS B226 (1989).

[7] Embid, R. Fernández, J.M. García-Sanz, and E. González. Estudio de la multiplicación neutrónica neta de un sistema ADS basado en plomo en función de la altura del haz de protones. Proceeding of the 24th Annual Meeting of the Spanish Nuclear Society at Valladolid, section 10-04 (1998).

[8] Fernández and E. González, Study on the Homogeneus and Heterogeneus Geometry Approaches for a Montecarlo Neutronic Calculation of the Energy Amplifier, CIEMAT REPORT 834 (1997).

[9] Embid, R. Fernández, J.M. García-Sanz, and E. González. Sensibilidad de la multiplicación neutrónica de un sistema ADS basado en plomo para su fuente de espalación en función de las librerías de secciones eficaces. Proceeding of the 24th Annual Meeting of the Spanish Nuclear Society at Valladolid, section 10-05 (1998).

[10] García-Sanz, M. Embid, R. Fernández and E.M. González. Estudio de K_{eff} para una geometría prototipo de ADS con combustibles de óxido de uranio. CIEMAT. DFN/TR-02/II-98 (1998).

[11] García-Sanz, M. Embid, R. Fernández y E. González. Cálculos neutrónicos para la definición de las primeras fases del laboratorio del amplificador de energía. CIEMAT. DFN/TR-04/II-98. (1998).

[12] García-Sanz, M. Embid, R. Fernández and E. González. Estudio de multiplicación neutrónica para un sistema subcrítico asistido por acelerador (ADS) con combustible de óxido de uranio y refrigerado por plomo. Proceeding of the 24th Annual Meeting of the Spanish Nuclear Society at Valladolid, section 10-11 (1998).

[13] Fernández, M. Embid, J.M. García-Sanz and E. González. Diseño de un procedimiento de simulación combinada de la evolución isotópica y neutrónica en un sistema subcrítico asistido por acelerador. Proceeding of the 24th Annual Meeting of the Spanish Nuclear Society at Valladolid, section 10-10 (1998).

[14] Fernández, M. Embid, J.M. García-Sanz and E. González. Performance on actinide transmutation of lead-thorium based ADS. Presented to this conference.